

†Research sponsored by the U. S. Atomic Energy Commission under contract with Union Carbide Corporation.

\*Present address: U. S. Atomic Energy Commission, Washington, D. C. 20545.

<sup>1</sup>H. C. Britt, H. E. Wegner, and J. C. Gursky, *Phys. Rev.* **129**, 2239 (1963).

<sup>2</sup>H. C. Britt and S. L. Whetstone, *Phys. Rev.* **133**, B603 (1964).

<sup>3</sup>J. P. Unik and J. R. Huizenga, *Phys. Rev.* **134**, B90 (1964).

<sup>4</sup>F. Plasil, D. S. Burnett, H. C. Britt, and S. G. Thompson, *Phys. Rev.* **142**, 696 (1966).

<sup>5</sup>E. Konecny and H. W. Schmitt, *Phys. Rev.* **172**, 1213 (1968), and E. Konecny, W. Nörenberg, and H. W. Schmitt, *Nucl. Phys.* **A139**, 513 (1969).

<sup>6</sup>I. F. Croall and J. G. Cuninghame, *Nucl. Phys.* **A125**, 402 (1969).

<sup>7</sup>P. P. D'Yachenko, B. D. Kuz'minov, and M. Z. Tarasko, *Yadern. Fiz.* **8**, 286 (1968) [transl.: *Soviet J. Nucl. Phys.* **8**, 165 (1969)].

<sup>8</sup>S. Baba, H. Umezawa, and H. Baba, *Nucl. Phys.* **A175**, 177 (1971).

<sup>9</sup>D. R. Nethaway and B. Mendoza, *Phys. Rev. C* **6**, 1827 (1972).

<sup>10</sup>See E. K. Hyde, *The Nuclear Properties of the Heavy Elements* (Prentice-Hall, Englewood Cliffs, N. J., 1964), Vol. III, and references therein.

<sup>11</sup>H. J. Specht, J. S. Fraser, and J. C. D. Milton, in *Proceedings of the International Nuclear Physics Con-*

*ference, Gallinburg, Tennessee, 1966* (Academic, New York, 1967), pp. 737-741; and J. C. D. Milton, J. S. Fraser, and H. J. Specht, *J. Phys. (Paris)* **2**, 17 (1972).

<sup>12</sup>W. Holubarsch, E. Pfeiffer, and F. Gönnerwein, *Nucl. Phys.* **A171**, 631 (1971).

<sup>13</sup>S. C. Burnett, R. L. Ferguson, F. Plasil, and H. W. Schmitt, *Phys. Rev. C* **3**, 2034 (1971).

<sup>14</sup>C. J. Bishop, R. Vandenbosch, R. Aley, R. W. Shaw, Jr., and I. Halpern, *Nucl. Phys.* **A150**, 129 (1970).

<sup>15</sup>J. R. Boyce, Ph.D. dissertation, Duke University, Durham, N. C., 1972 (unpublished).

<sup>16</sup>F. Pleasonton, *Phys. Rev.* **174**, 1500 (1968).

<sup>17</sup>H. W. Schmitt and F. Pleasonton, *Nucl. Instr. Methods* **40**, 204 (1966).

<sup>18</sup>F. Plasil, R. L. Ferguson, F. Pleasonton, and H. W. Schmitt, *Phys. Rev. C* **7**, 1186 (1973).

<sup>19</sup>H. W. Schmitt, W. E. Kiker, and C. W. Williams, *Phys. Rev.* **137**, B837 (1965); and H. W. Schmitt, W. M. Gibson, J. H. Neiler, F. J. Walter, and T. D. Thomas, in *Proceedings of the Symposium on the Physics and Chemistry of Fission, Salzburg, 1965* (International Atomic Energy Agency, Vienna, 1965), Vol. I, p. 531.

<sup>20</sup>H. W. Schmitt, J. H. Neiler, and F. J. Walter, *Phys. Rev.* **141**, 1146 (1966).

<sup>21</sup>A. Turkevich and J. B. Niday, *Phys. Rev.* **84**, 52 (1951).

<sup>22</sup>C. J. Bishop, I. Halpern, R. W. Shaw, Jr., and R. Vandenbosch, *Nucl. Phys.* **A198**, 161 (1972).

## Microscopic $^{130}\text{Ba}(n, \gamma)$ Cross Section and the Origin of $^{131}\text{Xe}$ on the Moon\*†

B. L. Berman and J. C. Browne

*Lawrence Livermore Laboratory, University of California, Livermore, California 94550*

(Received 27 October 1972)

The  $^{130}\text{Ba}(n, \gamma)$  cross section has been measured from 0.5 to 5000 eV with an energy resolution of 0.4%. The large epithermal resonances found in this experiment explain the anomalously high concentrations of  $^{131}\text{Xe}$  found in lunar rocks, and the measured resonance parameters provide one with a quantitative tool for correlating burial depth with exposure age for lunar samples.

### I. INTRODUCTION

Studies of lunar rocks<sup>1-6</sup> have revealed anomalously high concentrations of  $^{131}\text{Xe}$ , which apparently are associated with the cosmic-ray flux at the lunar surface, the depth (or shielding) history of the lunar samples involved, and the abundance of barium in these samples. Kaiser and Berman<sup>7</sup> have proposed that the explanation of this anomaly is the existence of a large, nonthermal-neutron-capture cross section for  $^{130}\text{Ba}$ , most likely in the resonance-energy region. They performed an integral measurement of this cross section by irradiating samples of natural barium with a linac-produced neutron source, whose en-

ergy spectrum was a good approximation to the neutron spectrum in the lunar regolith, and then measuring the neutron-produced  $^{131}\text{Xe}$  with a mass spectrometer. They concluded that the large average  $^{130}\text{Ba}(n, \gamma)$  cross section they obtained indeed could account for the " $^{131}\text{Xe}$  anomaly," but pointed out the need for a detailed microscopic cross-section measurement. This paper reports such a measurement.

### II. EXPERIMENT

A schematic diagram of the experimental apparatus is shown in Fig. 1. A pulsed 140-MeV electron beam from the Livermore linac (beam-pulse width 15 ns, repetition rate 720 pulses/s, peak

current 5 A) was directed upon a water-cooled tantalum neutron-producing target. The partially moderated neutrons, which passed through an evacuated and collimated 14.5-m flight tube, struck the  $(n, \gamma)$  sample, which was contained in a thin-walled aluminum can and positioned between a pair of 12.5-cm-diam by 7.5-cm-thick deuterated-benzene liquid-scintillator photon detectors, viewed by fast phototubes. Slabs of graphite, 2.5 cm thick, were placed between the sample and the detectors in order to make possible linear pulse-height weighting of the capture  $\gamma$ -ray signals (see below). The detectors subtended a total solid angle at the sample position of  $0.4 \times 4\pi$  sr.

Figure 2 shows a block diagram of the electron-

ics and data-collection system. The discriminator bias-level settings were adjusted, with the aid of various  $\gamma$ -ray sources, to a level corresponding to Compton electrons from 300-keV  $\gamma$  rays. Both the neutron time of flight and the linear pulse height for each event were stored on a magnetic drum in a two-dimensional array consisting of 20 000 time-of-flight channels by 64 pulse-height channels. A linear weighting function was applied to the pulse-height information in order to assure the spectral independence of the capture- $\gamma$ -ray detector efficiency,<sup>8-10</sup> and hence of the neutron-capture cross section obtained. We estimate that the uncertainty from this source remaining in the measured capture width for an individual reson-

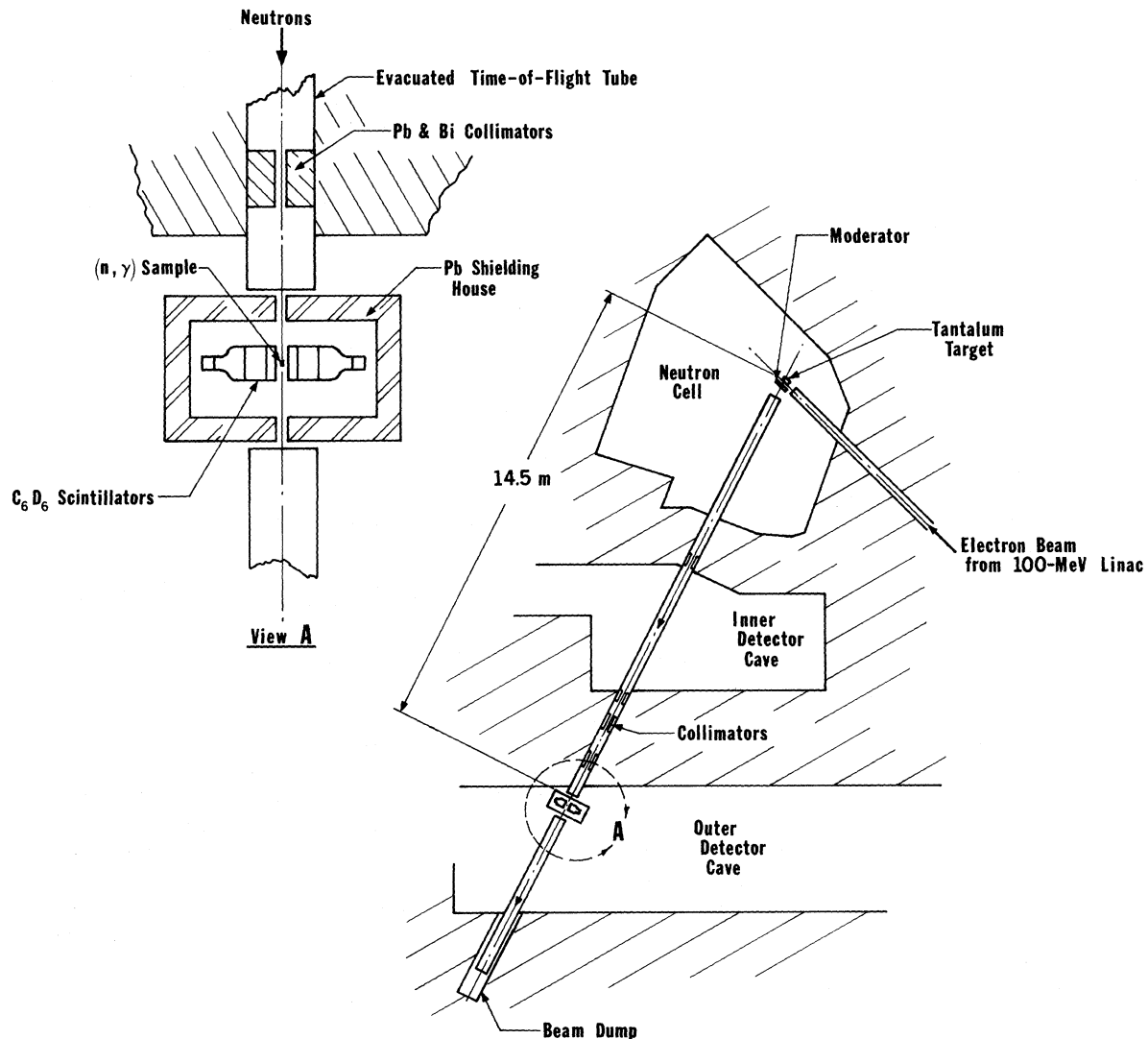


FIG. 1. Schematic diagram of the experiment. Neutrons produced when the pulsed electron beam from the linac strikes the tantalum target pass through the collimated flight tube and strike the  $(n, \gamma)$  sample, which is viewed, through graphite slabs, by a pair of liquid-scintillator photon detectors.

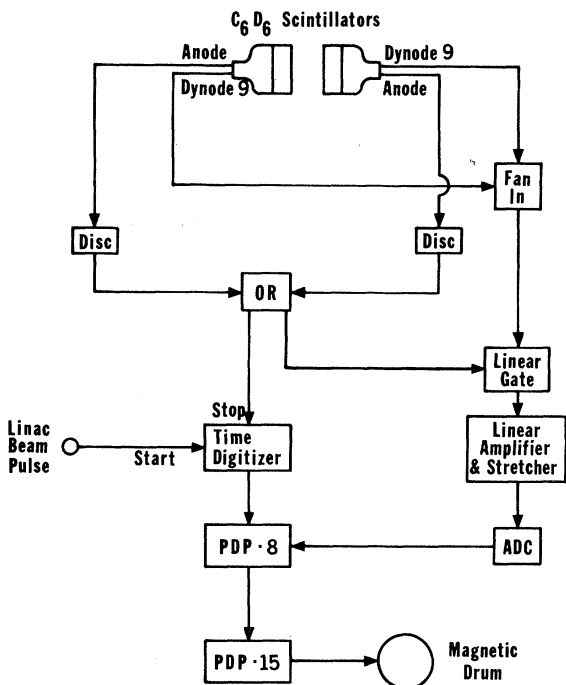


FIG. 2. Block diagram of the electronics and data-collection apparatus. Both neutron-time-of-flight and capture- $\gamma$ -pulse-height signals were stored in a two-dimensional array on the magnetic drum.

ance is at most 10%; for the integral cross section it is considerably less.

Although the nominal timing resolution was 1.5 ns/m, the experimental energy resolution was determined over a large range by the size of the neutron-producing target. The beam-burst width was so short that the uncertainty in the neutron time of flight does not contribute appreciably to the energy resolution below several keV, and the effects of the sample thickness and detector time resolution are negligible. The measured reso-

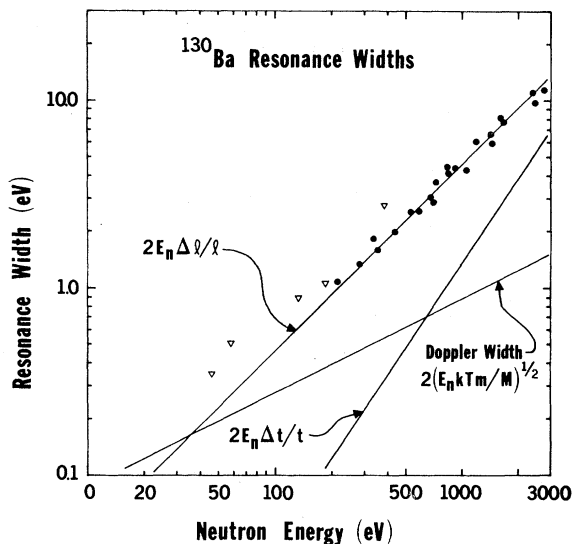


FIG. 3. Measured resonance widths plotted as a function of neutron energy. Contributions from Doppler broadening [ $2(E_n k T m / M)^{1/2}$ ], flight-path uncertainty ( $2E_n \Delta l / l$ ), and flight-time uncertainty ( $2E_n \Delta t / t$ ) are also shown. Including these effects we find five resolved resonances [shown as triangles ( $\nabla$ )] while all others are unresolved [shown as dots ( $\cdot$ )].

nance widths are plotted as a function of neutron energy in Fig. 3 along with the contributions to the widths from flight-path uncertainty, flight-time uncertainty, and Doppler broadening. From this plot, it can be seen that the resonances below about 200 eV are resolved.

Experimental runs were made with samples of enriched  $^{130}\text{Ba}$  and natural barium, both in the form of  $\text{Ba}(\text{NO}_3)_2$  powder. The masses of the samples were adjusted so that the number of  $^{135}\text{Ba}$  atoms in each sample was the same. The relative

TABLE I. Relative isotopic abundances and sample thicknesses.

Isotope	Enriched $^{130}\text{Ba}$ sample [2.37 g $\text{Ba}(\text{NO}_3)_2$ ]		Natural barium sample [2.24 g $\text{Ba}(\text{NO}_3)_2$ ]	
	Atomic percentage	Thickness ( $\text{g}/\text{cm}^2$ )	Atomic percentage	Thickness ( $\text{g}/\text{cm}^2$ )
130	37.05	0.064	0.101	0.00017
132	0.88	0.0015	0.097	0.00016
134	3.52	0.006	2.42	0.0041
135	6.34	0.010	6.59	0.011
136	5.55	0.0095	7.81	0.013
137	6.75	0.012	11.32	0.019
138	39.91	0.069	71.66	0.12

isotopic abundances and the thicknesses of the samples are given in Table I.

The energy dependence of the neutron flux was measured by using  $^{10}\text{B}$  as an experimental sample and making use of the  $E^{-1/2}$  dependence of the  $^{10}\text{B}(n, \alpha\gamma)$  cross section. For this run, a pulse-height window was set on the discriminators, in effect transforming them into single-channel analyzers, bracketing the 477-keV  $^{10}\text{B}$  reaction  $\gamma$  ray, and thus greatly reducing backgrounds from higher-energy  $\gamma$  rays. All the experimental runs were made with a 650-mg/cm<sup>2</sup>-thick cadmium filter in the neutron flight path. Use was made of the fact that the cadmium resonance at 89.6 eV, shown in Fig. 4, was completely black in the  $^{10}\text{B}$  run to show that backgrounds resulting from scattered neutrons, faulty collimation, ambient neutrons and  $\gamma$  rays, and the like, were small. The neutron energy scale was set with reference to the known resonances in  $^{135}\text{Ba}$ , cadmium, and aluminum, as well as a number of well-known resonances throughout the energy range of the experiment observed in a separate experimental run taken with a tantalum sample.

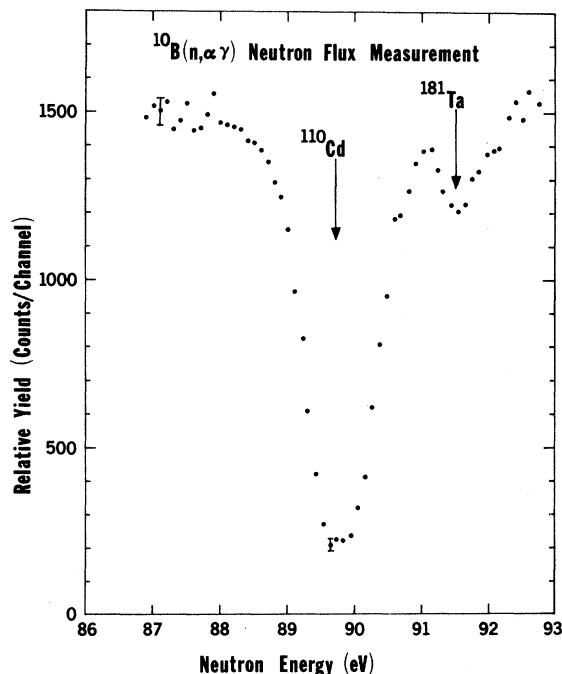


FIG. 4. A portion of the  $^{10}\text{B}$  neutron-spectrum run, showing the transmission dip at 89.6 eV resulting from the presence of the cadmium filter in the neutron flight path. Since no backgrounds have been subtracted from these data, the count rate at the transmission minimum is a measure of the background at that neutron energy.

### III. RESULTS

The present  $^{130}\text{Ba}(n, \gamma)$  cross-section results are shown in Fig. 5. Well-known<sup>11</sup> resonances in  $^{135}\text{Ba}$  at 24.4, 82, 88, 283, and 405 eV were used to normalize the  $^{130}\text{Ba}$  cross section. Resonances up to 2.5 keV were assigned to the various barium isotopes by comparing the areas under the resonances for both the enriched  $^{130}\text{Ba}$  and the natural barium samples. These isotopic assignments are listed in Table II.

There were 39 additional resonances observed between 2.5 and 5.0 keV. Although definite isotopic assignments were not made for these resonances, the majority must be either  $^{130}\text{Ba}$  or  $^{132}\text{Ba}$  resonances. The exception to this is a resonance at 4712 eV which was assigned to  $^{136}\text{Ba}$  [see Fig. 5(c)]. The values for  $g\Gamma_n\Gamma_\gamma/\Gamma$  listed in Table II were obtained for the  $^{130}\text{Ba}$  resonances from the area  $A$  under these resonances using the relation

$$A = 2\pi^2\lambda^2 g\Gamma_n\Gamma_\gamma/\Gamma, \quad (3.1)$$

where  $\lambda$  is the neutron wavelength and  $g$  is the statistical factor  $(2J+1)/[2(2I+1)]$  ( $J$  is the compound-state spin,  $I$  is the initial-state spin).

As shown in Fig. 3, there were five resolved resonances assigned to  $^{130}\text{Ba}$  in these data. For these resonances a total width,  $\Gamma$ , can be extracted by taking into account the effects of Doppler broadening, flight-path uncertainty, and flight-time uncertainty. If we assume that these five resonances are all  $s$  wave ( $l=0$ ,  $g=1$ ), then we can derive values for  $\Gamma_n$  and  $\Gamma_\gamma$  from  $\Gamma$  and the resonance area. Values derived for  $\Gamma_n$  and  $\Gamma_\gamma$  by this method are listed in Table III.

However, the other 35 resonances assigned to  $^{130}\text{Ba}$  in Table II were not resolved, so that values of  $\Gamma$  cannot be extracted directly from the data. Since the variation of  $\Gamma_\gamma$  from resonance to resonance should be small in this mass region, we can assume that  $\Gamma_\gamma$  is constant in order to extract values for  $\Gamma_n$  using Eq. (3.1). We assume that  $\bar{\Gamma}_\gamma = 100$  meV for  $^{130}\text{Ba}$ , similar to the measured average values of  $\bar{\Gamma}_\gamma$  for other nuclei in this mass region.<sup>12</sup> (This is also similar to the value of  $\bar{\Gamma}_\gamma = 95$  meV derived from our data in Table III.) We also assume that all resonances are  $s$  wave. The values of  $\Gamma_n$  thus extracted for all the resonances in the  $^{130}\text{Ba}(n, \gamma)$  cross section up to 2775 eV are listed in Table IV. It can be seen from both Tables III and IV that the uncertainties in the derived parameters are large, so that these widths probably should be used only to obtain average resonance parameters.

Although no previous microscopic neutron-capture measurement on  $^{130}\text{Ba}$  has been reported, there have been a few neutron total-cross-section



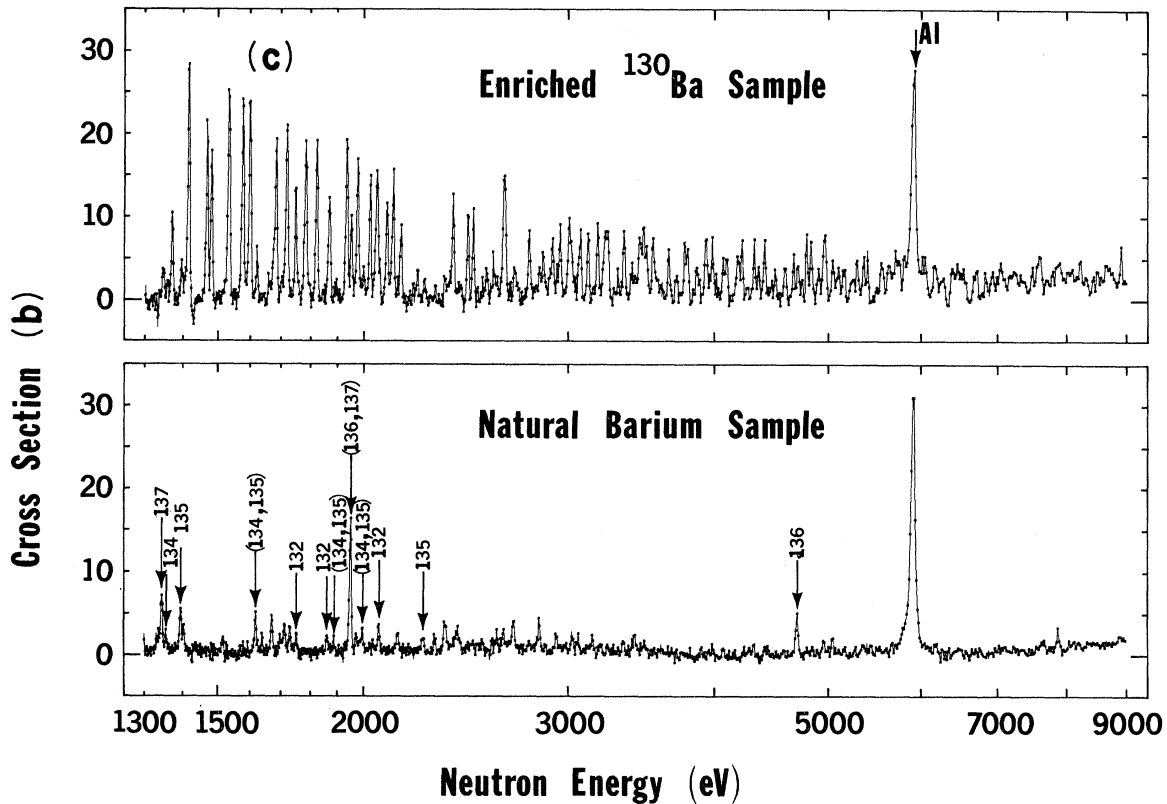


FIG. 5 (Continued)

measurements performed on barium isotopes,<sup>13-15</sup> one of them<sup>13</sup> with a sample somewhat enriched (14.4%) in  $^{130}\text{Ba}$ . Some results of these experiments can be compared with the resonance parameters presented here. For the 46.4-eV resonance, Vertebnyi *et al.*<sup>13</sup> report  $E_n = 46.6$  eV and  $\Gamma_n = 27$  meV; Van de Vijver and Pattenden<sup>15</sup> report  $E_n = 48.6$  eV and  $\Gamma_n = 30$  meV, but prefer an assignment to  $^{132}\text{Ba}$ ; and Alves *et al.*<sup>14</sup> report  $E_n = 46.2$  eV, but give no isotopic assignment. For the 58.0-eV resonance, Ref. 13 gives  $E_n = 58.2$  eV and  $\Gamma_n = 144$  meV; Ref. 14 gives  $E_n = 57.2$  eV,  $\Gamma_n = 190$  meV, and  $\Gamma_\gamma = 90$  meV, but assigns it to  $^{132}\text{Ba}$ ; and Ref. 15 gives  $E_n = 57.9$  eV and  $\Gamma_n = 164$  meV. Vertebnyi *et al.*<sup>13</sup> also saw resonances at 137 and 186 eV, corresponding to the present values for  $E_n$  of 136 and 185 eV, and give them a probable assignment to  $^{130}\text{Ba}$ . Alves *et al.*<sup>14</sup> assign six other resonances to  $^{130}\text{Ba}$  between 379 and 896 eV and give  $\Gamma_n$  values for them; we identify 10 resonances for  $^{130}\text{Ba}$  between 379 and 900 eV, but only two of these definitely correspond to ones reported in Ref. 14. Finally, both Refs. 14 and 15

assign to other barium isotopes a number of other resonances which correspond in energy to  $^{130}\text{Ba}$  resonances seen in this experiment; no doubt some of these have been misassigned. A comparison of the present results with these various data is given in Table II.

#### IV. DISCUSSION

The total area under the 40 resonances in the  $^{130}\text{Ba}(n, \gamma)$  cross section between 46.4 eV and 2.8 keV is approximately  $2.0 \times 10^4$  beV. From the resonance areas we can obtain a resonance absorption integral ( $R$ ), where it is defined as

$$R = \int_{E_1}^{E_2} [\sigma_\gamma(E)/E] dE, \quad (4.1)$$

where the limits of integration refer to the energy range of this experiment. We can approximate this integral by a sum over all the resonances as

$$R \approx \sum_i (1/E_i) \int \sigma_\gamma(E) dE = \sum_i (A_i/E_i), \quad (4.2)$$

since the energy,  $E$ , is essentially constant over

TABLE II. Isotopic assignments of resonances up to 2775 eV listed below were obtained from a comparison of enriched  $^{130}\text{Ba}$  and natural-barium-sample data. Values for  $g\Gamma_n\Gamma_\gamma/\Gamma$  for these resonances were obtained from resonance areas as discussed in the text.

$E_0$ (eV)	Present results		Previous assignments <sup>a</sup>		
	Assignment	$g\Gamma_n\Gamma_\gamma/\Gamma$ <sup>b</sup> (meV)	Ref. 15	Ref. 14	Ref. 13
24.4	135				
46.4	130	$29.0^{+8.7}_{-5.8}$	(130, 132)		130
58.0	130	$76.9 \pm 15.4$	(130, 132)	132	130
80.9	135				
86.2	135				
102.3	134				
104.2	132		135	135	
125.9	132		137		
136.2	130	$62.5^{+18.8}_{-12.5}$			130
184.5	130	$82.9 \pm 16.6$			130
213	130	$0.8 \pm 0.2$			
219	135				
224	135				
242 <sup>c</sup>	132		135		
283	135				
287	130	$26.5 \pm 5.3$			
316	135				
336	130	$50.3 \pm 10.0$			
358	130	$4.0 \pm 0.8$			
377	(135)				
380	130	$42.4 \pm 8.5$		130	
406	135				
420	(136, 137)		137	137	
425	132				
434	135				
445	130	$42.1 \pm 8.4$	136	130	
466	135				
500	132		134	134	
511	136				
558	130	$8.2 \pm 1.6$			
578	137				
582	130	$37.2 \pm 7.4$			
651	(136)			135	
653	(135)			135	
668	132		135		
698	130	$54.9 \pm 11.0$			
713	130	$29.8 \pm 6.0$			
723	(134)		135	135	
744	130	$60.3 \pm 12.1$			
832	d		135		
837	130	$65.8 \pm 13.2$			
850	130	$61.6 \pm 12.3$			
881	134		135	135	
893	132			130	
903	130	$45.5 \pm 9.1$			
942	(134, 135)			135	
948	132				
973	134				
1029	135				
1048	137				
1064	132				
1098	130	$74.2 \pm 14.8$	137		
1121 <sup>c</sup>	(134)				
1149	132				
1156	d		135		
1172	130	$77.7 \pm 15.5$			
1199	d		135		

TABLE II (Continued)

$E_0$ (eV)	Present results		Previous assignments <sup>a</sup>		
	Assignment	$g\Gamma_n \Gamma_\gamma / \Gamma$ <sup>b</sup> (meV)	Ref. 14	Ref. 13	Ref. 12
1205	132				
1224	(134)		134		
1250	130	4.6 ± 0.9			
1266	130	37.3 ± 7.5			
1276	135				
1348	137				
1359	134				
1371	132				
1397	135				
1406	d				
1416	130	66.1 ± 13.2			
1468	130	54.1 ± 10.8			
1482	130	41.9 ± 8.4			
1534	130	81.0 ± 16.2			
1576	130	83.2 ± 16.6			
1599	130	84.4 ± 16.9			
1621 <sup>c</sup>	(134, 135)				
1641	d		136		
1672	d				
1685	130	80.7 ± 16.1			
1715	d				
1721	130	90.9 ± 18.2			
1750	132				
1784	130	89.8 ± 18.0			
1824	130	76.2 ± 15.2			
1871	132		135		
1890	(134, 135)		134		
1934	130	102.1 ± 20.4			
1952	(136, 137)				
1977	132				
1998	(134, 135)		135		
2029	132				
2054	132				
2095	130	64.3 ± 12.9			
2121	130	83.3 ± 16.7			
2155	130	58.2 ± 11.6			
2227	(130)				
2256	135				
2387	(130)	85.0 ± 17.0			
2456	(130)	75.4 ± 15.1			
2486	(130)	67.2 ± 13.4			
2775	(130)	61.3 ± 12.3			

<sup>a</sup> Assignments are listed only where they disagree with present results or where relevant comparisons can be made.

<sup>b</sup> Experimental error includes uncertainties in pulse-height weighting, cross-section normalization, background subtraction, and flux determination.

<sup>c</sup> Possible doublet.

<sup>d</sup> Could not be assigned from the present data alone.

the narrow resonances in the  $^{130}\text{Ba}(n, \gamma)$  cross section. For the above energy range, we therefore obtain a value for  $R$  equal to  $180_{-40}^{+60}$  b. The total uncertainty in this number includes the uncertainties resulting from pulse-height weighting, cross-section normalization, and background subtraction.

To explain the excess  $^{131}\text{Xe}$  found in Apollo-12

lunar rocks, Schwaller *et al.*<sup>16</sup> estimated that the resonance integral for the  $^{130}\text{Ba}(n, \gamma)$  cross section must be at least 150 b. This result was derived from cosmic-ray fluxes and the neutron slowing-down density of lunar material. Considering the complexity of understanding the lunar history of a sample, the agreement between our results and

TABLE III. Neutron and total radiation widths for resolved  $^{130}\text{Ba}$  resonances. These widths were obtained from resonance areas under the assumption that  $l=0$  ( $g=1$ ) for these resonances. Uncertainties in  $\Gamma_n$  and  $\Gamma_\gamma$  are correlated as can be seen from Eq. (3.1).

Present results				Previous measurements $\Gamma_n$ (meV)
$E_0$ (eV)	$\Gamma_\gamma$ (meV) <sup>a</sup>	$\Gamma_n$ (meV)	$\Gamma_n^0$ (meV) <sup>b</sup>	
46.4	122 ± 65	38 ± 20	5.6	27 <sup>c</sup>
58.0	110 ± 38	250 ± 85	32.8	144 <sup>c</sup>
136.2	80 ± 26	300 ± 100	25.7	
184.5	130 ± 107	230 ± 190	16.9	
380	45 ± 5	1475 ± 140	75.7	1390 <sup>d</sup>

<sup>a</sup> The average value of  $\bar{\Gamma}_\gamma$  calculated from the first four resonances is 95 ± 20 meV.

<sup>b</sup> Reduced neutron width,  $\Gamma_n^0 = \Gamma_n (E_n)^{-1/2}$ .

<sup>c</sup> Reference 13.

<sup>d</sup> Reference 14.

the above estimate is very good. It is clear that the quantitative results of the present measurement, along with the earlier and more qualitative measurements of Kaiser and Berman,<sup>7</sup> show that the  $^{130}\text{Ba}(n, \gamma)$  reaction indeed is almost surely the source of the excess  $^{131}\text{Xe}$  found in the lunar samples. This knowledge of the  $^{130}\text{Ba}$  capture cross section therefore provides the key link for correlating burial depth with exposure age for lunar samples.

#### ACKNOWLEDGMENTS

We would like to thank Dr. C. D. Bowman and Dr. J. B. Czirr for useful discussions throughout the experiment.

TABLE IV. Neutron widths obtained for  $^{130}\text{Ba}$  resonances under the assumptions that  $\Gamma_\gamma = \text{constant}$  (100 meV) and that all resonances are s wave ( $g=1$ ).

$E_0$ (eV)	$\Gamma_n$ (meV)	$\Gamma_n^0$ (meV) <sup>a</sup>	$E_0$ (eV)	$\Gamma_n$ (meV)	$\Gamma_n^0$ (meV)
46.4	41 ± 11 <sup>†</sup>	5.9	1250	5 ± 1	0.2
58.0	330 ± 300	21.0	1266	60 ± 20	1.7
136.2	170 ± 140	42.4	1416	195 ± 115	5.2
184.5	480 ± 480	14.7	1468	120 ± 50	3.1
213	1 ± 0.3	0.1	1482	75 ± 25	2.0
287	36 ± 10	2.1	1534	425 ± 425	10.9
336	105 ± 40	5.7	1576	500 ± 500	12.6
358	4 ± 1	0.2	1599	540 ± 540	13.5
380	75 ± 25 <sup>b</sup>	3.9	1685	420 ± 420	10.2
445	75 ± 25	3.6	1721	1000 ± 1000	24.1
558	10 ± 2	0.4	1784	880 ± 880	20.8
582	60 ± 20	2.5	1824	320 ± 270	7.5
698	125 ± 55	4.7	1934	c	
713	45 ± 15	1.7	2095	180 ± 100	3.9
744	155 ± 80	5.7	2121	500 ± 500	10.9
837	195 ± 115	6.7	2155	140 ± 65	3.0
850	160 ± 80	5.5	2387	570 ± 570	11.7
903	85 ± 30	2.8	2456	305 ± 250	6.2
1098	290 ± 225	8.8	2486	205 ± 125	4.1
1172	350 ± 310	10.2	2775	160 ± 80	3.0

<sup>a</sup> Reduced neutron width,  $\Gamma_n^0 = \Gamma_n (E_n)^{-1/2}$ .

<sup>b</sup> Notice that assumption of  $\Gamma_\gamma = 100$  meV leads to large discrepancy for  $\Gamma_n$  between Tables III and IV.

<sup>c</sup> Could not be determined by this method.

\*Work performed under the auspices of the U.S. Atomic Energy Commission.

<sup>†</sup>A preliminary account of this work appeared as Bull. Am. Phys. Soc. **17**, 529 (1972).

<sup>1</sup>C. M. Hohenberg, P. K. Davis, W. A. Kaiser, R. S. Lewis, and J. H. Reynolds, in *Proceedings of the Apollo II Lunar Science Conference*, edited by A. A. Levinson (Pergamon, New York, 1970), Vol. 2, p. 1283.

<sup>2</sup>K. Marti, G. W. Lugmair, and H. C. Urey, in *Proceedings of the Apollo II Lunar Science Conference*, edited by A. A. Levinson (Pergamon, New York, 1970), Vol. 2, p. 1357.

<sup>3</sup>R. O. Pepin, L. E. Nyquist, D. Phinney, and D. C. Black, in *Proceedings of the Apollo II Lunar Science Conference*, edited by A. A. Levinson (Pergamon, New York, 1970), Vol. 2, p. 1435.

<sup>4</sup>A. L. Albee, D. S. Burnett, A. A. Chodos, O. J. Eugster, J. C. Huneke, D. A. Papanastassiou, F. A. Podosek, G. Price Russ, III, H. G. Sanz, F. Tera, and G. J. Wasserburg, *Science* **167**, 463 (1970).

<sup>5</sup>P. Eberhardt, J. Geiss, H. Graf, N. Grögler, U. Krähenbühl, H. Schwaller, J. Schwarzmüller, and A. Stettler, *Earth Planet. Sci. Lett.* **10**, 67 (1970).

<sup>6</sup>W. A. Kaiser, in *Proceedings of the Second Lunar Scientific Conference*, edited by A. A. Levinson (MIT Press, Cambridge, 1971), Vol. 2, p. 1627.

<sup>7</sup>W. A. Kaiser and B. L. Berman, in *Proceedings of the Third Lunar Scientific Conference*, Houston, 1972, edited by C. Watkins, Lunar Science Institute Document LC-79-189790, p. 444; B. L. Berman and W. A. Kaiser, *Bull. Am. Phys. Soc.* **17**, 17 (1972); W. A. Kaiser and B. L. Berman, *Earth Planet. Sci. Lett.* **15**, 320 (1972).

<sup>8</sup>G. S. Hurst and R. H. Ritchie, *Health Phys.* **8**, 117 (1962).

<sup>9</sup>R. L. Macklin and J. H. Gibbons, *Phys. Rev.* **159**, 1007 (1967).

<sup>10</sup>J. B. Czirr, *Nucl. Instrum. Methods* **72**, 23 (1969).

<sup>11</sup>*Neutron Cross Sections*, compiled by M. D. Goldberg, S. F. Mughabghab, S. N. Purohit, B. A. Magurno, and V. M. May, Brookhaven National Laboratory Report No. BNL-325 (U. S. GPO, Washington, D. C., 1966), 2nd. ed., 2nd Suppl.

<sup>12</sup>J. E. Lynn, *Theory of Neutron Resonance Reactions* (Clarendon Press, Oxford, England, 1968), p. 318.

<sup>13</sup>V. P. Vertebnyi, A. I. Kal'chenko, M. V. Pasechnik, and Zh. I. Pisanko, *Ukr. Fiz. Zh.* **14**, 227 (1969).

<sup>14</sup>R. N. Alves, S. DeBarros, P. L. Chevillon, J. Julien, J. Morgenstern, and C. Samour, Nucl. Phys. A134, 118 (1969).

<sup>15</sup>R. E. Van de Vijver and N. J. Pattenden, Nucl. Phys.

A177, 393 (1971).

<sup>16</sup>H. Schwaller, P. Eberhardt, J. Geiss, H. Graf, and N. Grögler, Earth Planet. Sci. Lett. 12, 167 (1971).

PHYSICAL REVIEW C

VOLUME 7, NUMBER 6

JUNE 1973

## How Good Are the Theoretical Internal-Conversion Coefficients?\*

S. Raman and T. A. Walkiewicz<sup>†</sup>

*Oak Ridge National Laboratory, Oak Ridge, Tennessee 37830*

R. Gunnink

*Lawrence Livermore Laboratory, Livermore, California 94550*

B. Martin

*Max-Planck-Institut für Kernphysik, Heidelberg, Germany*

(Received 12 February 1973)

We have accurately measured the total-conversion coefficient for the 156.0-keV,  $M4$  transition in  $^{117}\text{Sn}$  as  $\alpha_T = 46.40 \pm 0.25$ . The Hager and Seltzer theoretical value is 47.8. A comparison between experimental and theoretical  $\alpha_K$  and  $\alpha_T$  values for 15  $E3$  and  $M4$  transitions shows that the theoretical values are systematically 2–3% higher.

### I. INTRODUCTION

It is generally believed that the theory of internal conversion is in broad agreement with experiment. There exist several tabulations of calculated internal-conversion coefficients. Basically, these calculations require a knowledge of the bound-state and continuum electron wave functions. In the tables of Hager and Seltzer,<sup>1</sup> the wave functions are relativistic Hartree-Fock-Slater solutions to the Dirac equation.

To estimate the uncertainties in any calculation is difficult. It is difficult enough to assess the influence of physically reasonable variations in the assumptions that go into any calculation (what is the correct screening function or nuclear charge distribution? – is a central potential or nonrelativistic treatment adequate? – etc.), not to speak of several “one-percent effects” that are altogether omitted (higher-order terms in the fine-structure constant, static nuclear multipole moments, penetration effects, chemical shifts, electron correlations, etc.). What, in particular, is the combined effect of all these effects? To answer these questions indirectly, we have resorted to the philosophy, “The test of all knowledge is experiment,” expressed succinctly by Feynman, Leighton, and Sands.<sup>2</sup>

### II. EXPERIMENTAL PROCEDURE AND RESULTS

To test the theory to say 1%, we of course need a conversion-coefficient ( $\alpha$ ) measurement that

we can trust to the same accuracy. When an isomer deexcites via two transitions in cascade, it is possible to deduce the  $\alpha_T$  ratio by measuring photon intensities only<sup>3</sup>—a measurement inherently capable of better than 1% accuracy. Consider the case of 14-day  $^{117}\text{Sn}^m$  decay shown in Fig. 1. The 156.0-keV ( $\gamma_1$ ) transition is known to be  $M4$ ,<sup>4</sup> and the 158.6-keV ( $\gamma_2$ ) transition  $M1 + <0.05\% E2$ .<sup>5</sup> We can write

$$I_{\gamma_1}(1 + \alpha_{1T}) = I_{\gamma_2}(1 + \alpha_{2T}), \quad \alpha_T = I_{ce}/I_{\gamma}.$$

If the photon-intensity ratio  $I_{\gamma_2}/I_{\gamma_1}$  is measured and if  $\alpha_{2T}$  is small (say  $<0.2$ ) and set equal to the experimental or theoretical value,  $\alpha_{1T}$  can be readily obtained. The crucial point is that any percentage uncertainty in  $\alpha_{2T}$  is reduced by a factor  $\alpha_{2T}/(1 + \alpha_{2T})$  in the determination of  $\alpha_{1T}$ .

The 156.0–158.6-keV  $\gamma$ -ray doublet, well resolved with a 1.0-cm<sup>3</sup> Ge(Li) x-ray detector, is shown in Fig. 1. The  $^{117}\text{Sn}^m$  sources were produced by the  $^{118}\text{Sn}(n, 2n)$  reaction with 14-MeV neutrons. 13 spectra were recorded with two different detectors, two analyzers, and two irradiated  $^{118}\text{Sn}$  foils (0.51 and 1.52 mm thick).

Bearing in mind that we are interested only in the relative photopeak areas, an iterative self-consistent analysis of each spectrum was carried out with the same shape functions (a smoothed-step function to represent the background continuum + a Gaussian term + a tailing term) employed to represent both peaks. Apart from statistical and curve-fitting uncertainties (typically 0.2–0.3%